

SANDIA REPORT

SAND2001-1762

Unlimited Release

Printed September 2001

Capacity of Prestressed Concrete Containment Vessels with Prestressing Loss

Jeffrey A. Smith

Prepared by
Sandia National Laboratories
Albuquerque, New Mexico 87185 and Livermore, California 94550

Sandia is a multiprogram laboratory operated by Sandia Corporation,
a Lockheed Martin Company, for the United States Department of
Energy under Contract DE-AC04-94AL85000.

Approved for public release; further dissemination unlimited.



Sandia National Laboratories

Issued by Sandia National Laboratories, operated for the United States Department of Energy by Sandia Corporation.

NOTICE: This report was prepared as an account of work sponsored by an agency of the United States Government. Neither the United States Government, nor any agency thereof, nor any of their employees, nor any of their contractors, subcontractors, or their employees, make any warranty, express or implied, or assume any legal liability or responsibility for the accuracy, completeness, or usefulness of any information, apparatus, product, or process disclosed, or represent that its use would not infringe privately owned rights. Reference herein to any specific commercial product, process, or service by trade name, trademark, manufacturer, or otherwise, does not necessarily constitute or imply its endorsement, recommendation, or favoring by the United States Government, any agency thereof, or any of their contractors or subcontractors. The views and opinions expressed herein do not necessarily state or reflect those of the United States Government, any agency thereof, or any of their contractors.

Printed in the United States of America. This report has been reproduced directly from the best available copy.

Available to DOE and DOE contractors from
U.S. Department of Energy
Office of Scientific and Technical Information
P.O. Box 62
Oak Ridge, TN 37831

Telephone: (865)576-8401
Facsimile: (865)576-5728
E-Mail: reports@adonis.osti.gov
Online ordering: <http://www.doe.gov/bridge>

Available to the public from
U.S. Department of Commerce
National Technical Information Service
5285 Port Royal Rd
Springfield, VA 22161

Telephone: (800)553-6847
Facsimile: (703)605-6900
E-Mail: orders@ntis.fedworld.gov
Online order: <http://www.ntis.gov/ordering.htm>



SAND2001-1762
Unlimited Release
Printed September 2001

Capacity of Prestressed Concrete Containment Vessels with Prestressing Loss

Jeffrey A. Smith
Nuclear Technology Programs Department
Sandia National Laboratories
P.O. Box 5800
Albuquerque, NM 87185-0744

Abstract

Reduced prestressing and degradation of prestressing tendons in concrete containment vessels were investigated using finite element analysis of a typical prestressed containment vessel. The containment was analyzed during a loss of coolant accident (LOCA) with varying levels of prestress loss and with reduced tendon area. It was found that when selected hoop prestressing tendons were completely removed (as if broken) or when the area of selected hoop tendons was reduced, there was a significant impact on the ultimate capacity of the containment vessel. However, when selected hoop prestressing tendons remained, but with complete loss of prestressing, the predicted ultimate capacity was not significantly affected for this specific loss of coolant accident. Concrete cracking occurred at much lower levels for all cases. For cases where selected vertical tendons were analyzed with reduced prestressing or degradation of the tendons, there also was not a significant impact on the ultimate load carrying capacity for the specific accident analyzed. For other loading scenarios (such as seismic loading) the loss of hoop prestressing with the tendons remaining could be more significant on the ultimate capacity of the containment vessel than found for the accident analyzed. A combination of loss of prestressing and degradation of the vertical tendons could also be more critical during other loading scenarios.

Acknowledgment

The U.S. Nuclear Regulatory commission (NRC) sponsored this research program. The author acknowledges the contributions of others who were instrumental in the development of this research. Jeffery L. Cherry was the principal investigator at Sandia National Laboratories for the Degraded Containments Program for the majority of the time this work was being completed and helped initiate the scope of the work. Herman Graves, Wallace Norris, and James Costello, all of the NRC, also made significant contributions toward project development.

Contents

1. Introduction	8
2. Finite Element Model	10
2.1 Material Properties	11
2.2 Loading.....	13
2.3 Failure Criteria.....	14
3. Finite Element Runs and Results	19
3.1 Finite Element Runs	19
3.2 Results	21
3.2.1 Results in Terms of Ultimate Capacity	22
3.2.2 Other Trends	24
3.2.3 Observations	24
4. Conclusions	27
5. References	27

Figures

Figure 2-1. Schematic of Typical Prestressed Containment.	10
Figure 2-2. Typical Wall Layout of Prestressing Tendon and Reinforcing Bar.....	11
Figure 2-3. Finite Element 3D Mesh of 30° Segment of the Containment.....	11
Figure 2-4. Liner Material Stress-Strain Curves.....	12
Figure 2-5. Temperature Pressure Relationship.....	13

Tables

Table 2-1. Concrete Properties.....	12
Table 2-2. Reinforcing Bar and Prestressing Tendon Stress-Strain Properties	13
Table 3-1. Analysis Case	20
Table 3-2. Results for the Baseline and Uniform Degradation Cases.....	21
Table 3-3. Results for the Baseline and Degraded Vertical Tendons	22
Table 3-4. Results for the Baseline and Degraded Hoop Tendons	22

This page intentionally left blank.

1. Introduction

Prestressed concrete containments have numerous potential degradation sites. The concrete can degrade, and prestressing tendons, reinforcing bars, and the liner can corrode. A previous study by Cherry and Smith (2001) examined liner degradation of steel and concrete containments. The following study examines a typical prestressed concrete containment with degradation of prestressing levels during a loss of coolant accident (LOCA). Although concrete reinforcing bar degradation is a potentially serious condition, that accident scenario is beyond the scope of this project.

Regulations require that the prestressing tendons of the containment be inspected at 1, 3, and 5 years after the initial structural integrity test and every five years thereafter (Nuclear Regulatory Commission [NRC], 1990). Inservice inspections have found degradation of tendons. Therefore, there is a need to determine the impact degraded tendons have on the performance of the containment.

Degradation of prestressing can result from corrosion of the tendons, corrosion of the tendon anchor and/or degradation of the concrete at the anchor, stress relaxation of the prestressing steel, and from effects of high temperatures near the tendons. In addition to general corrosion, the tendons are also susceptible to pitting, stress corrosion cracking, and hydrogen embrittlement.

Stress corrosion cracking occurs when there is the combination of high tensile stress, susceptible material, and an aggressive environment. Hydrogen embrittlement (also referred to as hydrogen-assisted cracking) occurs when hydrogen is absorbed within the metal and interacts with defects in the steel, creating a loss of ductility. Hydrogen can be introduced into the steel during fabrication or as a byproduct of corrosion. Shah and Hookham (1998) offer more detailed descriptions of each of these degradation types.

Shah and Hookham (1998) discuss tendon corrosion from hydrogen embrittlement, general corrosion, and stress corrosion cracking detected in a number of plants. They concluded that corrosion has resulted of water accumulating at the lower ends of the vertical tendons in the area of the anchorage, and poor construction practices. Tendons that have been stored on site for long periods with no protection or that have not been properly protected once installed, but prior to the application of permanent corrosion protection, can have degradation.

Ashar et al. (1994) also discuss findings of containments with lower than expected prestressing levels. In one case, several hoop tendons' prestressing levels measured at three years after post-tensioning were lower than levels predicted to occur after 40 years. Also, vertical tendons were found with excessive loss of prestressing during inspections that occurred about 13 years after post-tensioning. Ashar et al. (1994) suggested that contributing factors were improper calibration of the jacks during the initial post-tensioning, higher than expected assumed losses, and failures in quality control.

An information notice released by the NRC (1999) discusses degradation of prestressing tendon systems in prestressed concrete containments at two plants: one from broken wires, the other

from anchor-head failure). The lower than expected prestressing levels from higher than expected average temperatures around the tendons are also considered (NRC, 1999).

Norris et al. (1999) discuss the possibility that the actual minimum force in the tendons may be lower than that calculated from the anchorage force, implying that the time-dependent losses along a tendon length could be higher than at the end anchorages. Steinberg (1995) gives numerical examples that show the variability of the prestress losses exceeds the losses calculated by deterministic methods. Therefore, “tendon degradation,” whether from actual degradation of the tendon, lower than expected prestressing levels, or higher than expected prestressing losses, should to be investigated.

Shah and Hookham (1998) stated that prestress losses detected at the 20- and 25-year tendon inspections exceeded those predicted for 40 years. One of their main concerns is that loss of prestress is loss of load-carrying capacity of the containment.

The following study examines how much load-carrying capacity is lost and how the level of loss and pattern of degraded tendons affects the loss of capacity. This study examines the effects of tendon degradation on the ultimate load-carrying capacity of the containment under a LOCA accident. A typical pressurized-water reactor (PWR) prestressed concrete containment was examined using finite element (FE) analysis with postulated tendon degradation. The containment modeled is similar to the Zion nuclear power station containment. The dimensions, liner thickness, reinforcing bars’ spacing and size, prestressing tendon spacing and sizes, were all taken from structural drawings of the containment at the Zion containment. However, the level of tendon degradation and locations of tendon degradation were chosen independent of any known degradation in the containment at the Zion nuclear power station.

2. Finite Element Model

A schematic of the typical prestressed concrete containment modeled in the finite element (FE) analysis is shown in Figure 2-1. The containment's inside diameter is 42.67 m (140 ft); inside height is 64.62 m (212 ft). The wall thickness in the cylinder is 1.07 m (3.5 ft), 0.81 m (2.67 ft) in the dome, and the steel liner is 6.35 mm (0.25 in) thick. The concrete basemat thickness is typically 2.74 m (9 ft) thick. Figure 2-2 shows the typical wall layout of the reinforcing bars and prestressing tendons.

The ABAQUS finite element code (ABAQUS, 1997) was used in the analysis. ABAQUS, a general-purpose finite element code, provides the option to use external material models. In this study the behavior of the concrete material was modeled using ANACAP_U (ANATECH Corp., 1997). This material model uses the smeared-crack approach (Rashid, 1968) to model the cracking concrete. Details of the concrete material model can be found in Appendix A of James et al. (1999)

Symmetry conditions were used to reduce the model to a 30° segment of the containment. This segment runs from the centerline of one of the six buttresses to half the distance between two of the buttresses. To simplify the model, the equipment hatch was not modeled. Figure 2-3 shows the finite element 3D mesh. 20-node brick elements were used to model the concrete, and 8-node shell elements were used to model the liner. The liner was attached to the concrete at the common nodes. The hoop and dome tendons were modeled as reinforcing bars and, thus, in the model they are bonded to the concrete. The vertical tendons were modeled using truss elements and are attached at four points along their lengths (i.e., see Figure 2-3). These vertical tendons are not bonded to the concrete, except at attachment points. Springs were used on the base of the model to allow uplift at the basemat.

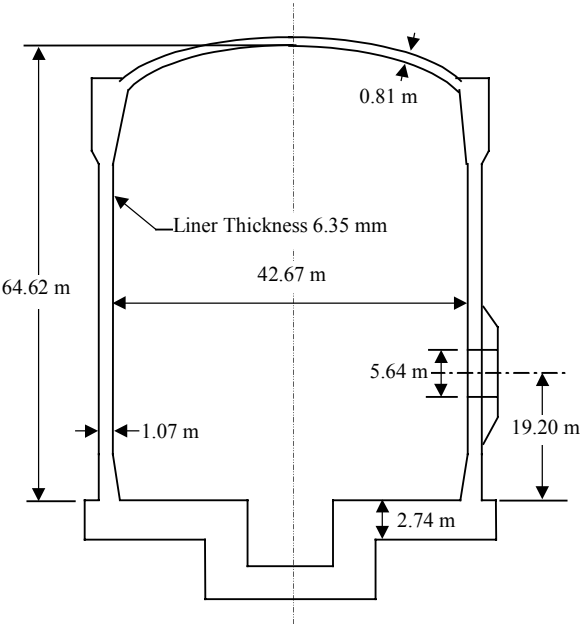


Figure 2-1. Schematic of Typical Prestressed Concrete Containment.

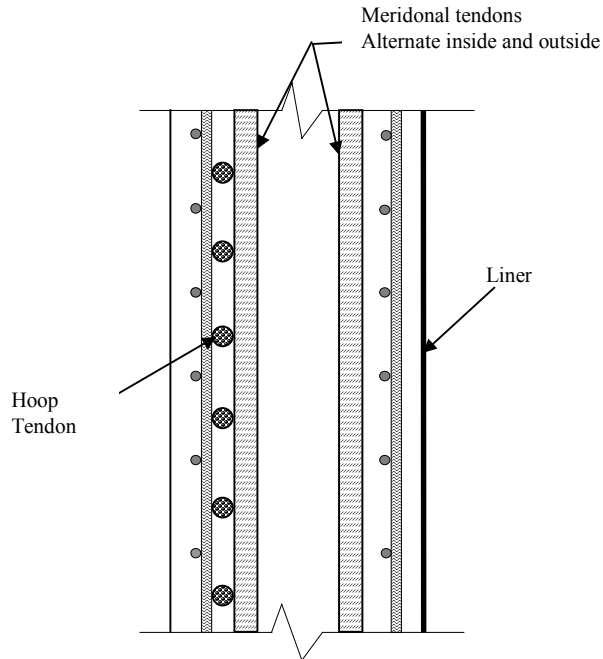


Figure 2-2. Typical Wall Layout of Prestressing Tendon and Reinforcing Bar.

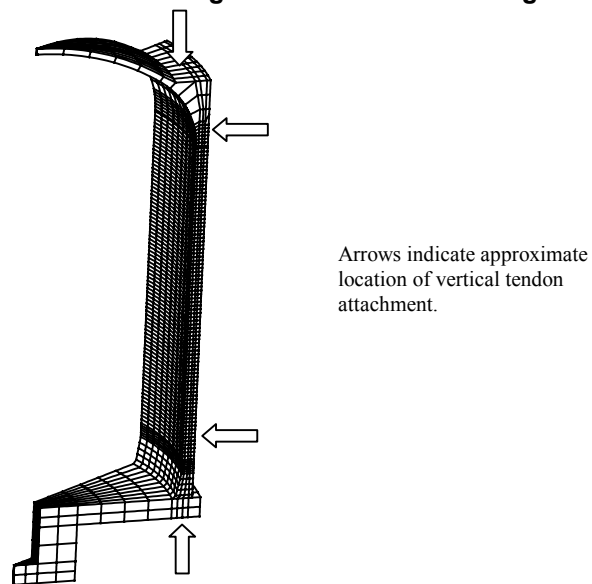


Figure 2-3. Finite Element 3D Mesh of 30° Segment of the Containment.

2.1 Material Properties

The liner material properties used in the FE model were for A516 Grade 60 steel. The true stress-strain curve is shown in Figure 2-4. This curve was developed by using a mean value of engineering yield and ultimate stress from test data obtained from the containment liner at the Sequoyah nuclear power station. The curve was developed to be proportional to curves for A516 Grade 70 steel tested at 22°C (Fatigue Technology, Inc., 1988). Engineering stress and strain val

ues were converted to true stress and true strain, which are required by the FE code to define plastic material properties.

Table 2-1 shows material properties used for the concrete. These values are the as-built material properties of the concrete in the base slab and above the base slab from Butler and Fugelso (1982). The material properties for reinforcing bars and prestressing tendons were taken from Weatherby (1988)¹ and are shown in Table 2-2.

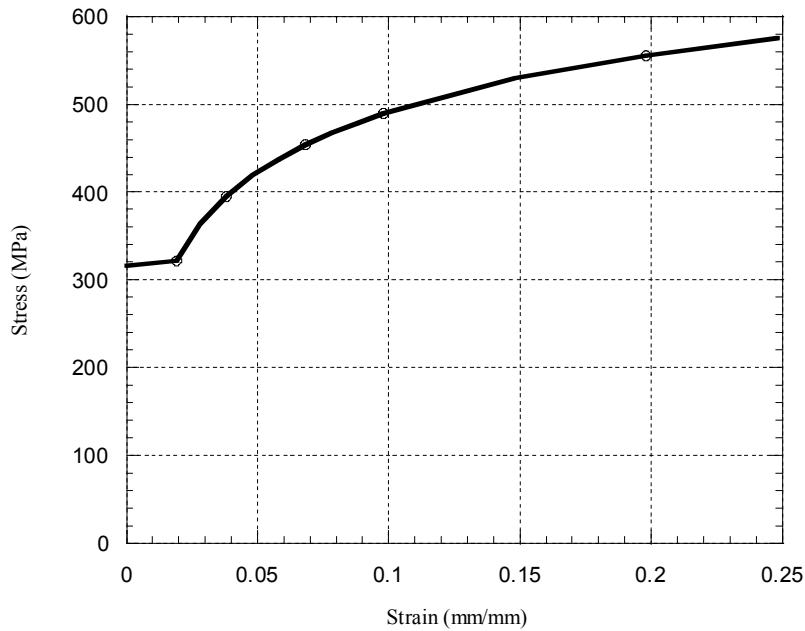


Figure 2-4. Liner Material Stress-Strain Curves.

Table 2-1. Concrete Properties

	Above Base Slab	Base Slab
Uniaxial Maximum Compressive Stress (f'_c)	45.5 MPa (6,600 psi)	40.7 MPa (5,900 psi)
Poisson's Ratio	0.19	0.19
Modulus of Elasticity	39.3 GPa (5.7×10^6 psi)	34.5 GPa (5.0×10^6 psi)

¹ Weatherby, J.R. 1988. "Structural Assessments of the Surry and Zion Reactor Containment Buildings for NUREG-1150," memorandum to R.J. Breeding, Sandia National Laboratories, Albuquerque, NM.

Table 2-2. Reinforcing Bar and Prestressing Tendon Stress-Strain Properties

Reinforcing Bars		Prestressing Tendons	
Yield Stress MPa (psi)	Strain %	Yield Stress MPa (psi)	Strain %
0.46 (66.6)	0.23	1.45 (210.0)	0.78
0.50 (73.3)	1.18	1.52 (220.0)	1.0
0.59 (85.6)	2.27	1.66 (240.0)	5.0
0.68 (99.0)	4.01		
0.72 (105.0)	10.0		

2.2 Loading

The FE model was loaded with a quasi-static internal pressure that increased monotonically. During many postulated accidents, the pressure is caused by water turning into steam. The saturated steam temperature-pressure relationship is shown in Figure 2-5. The pressure load applied to the FE model is applied as described by this curve.

Although many possible accident scenarios exist and are important near design pressures, for the calculation of ultimate capacity of the containment under internal pressure, the thermal loads do not have a significant effect. The effects of thermal loads on the liner strains are dissipated as the concrete cracks and reinforcing bars yield. Therefore, for this study the thermal loads were ignored.

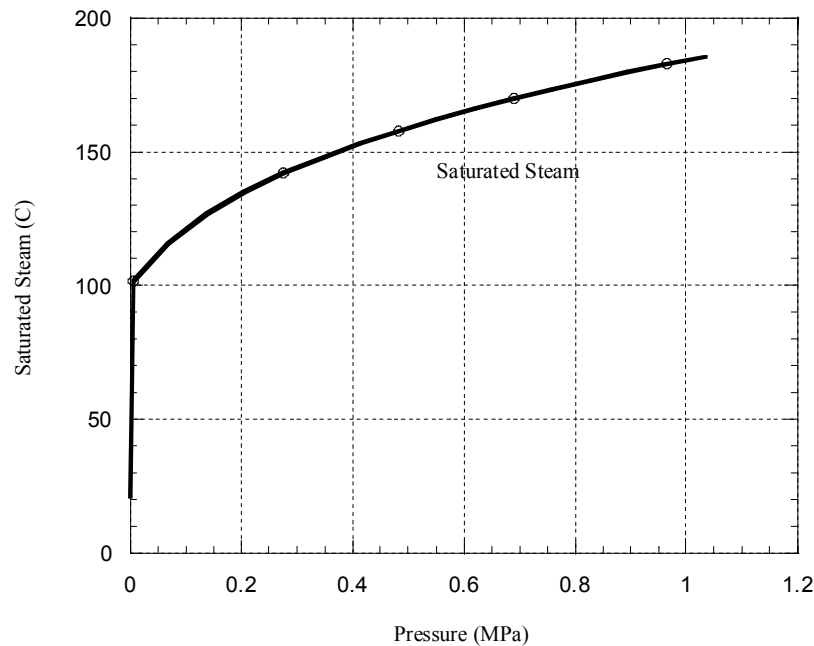


Figure 2-5. Temperature Pressure Relationship.

2.3 Failure Criteria

The primary mode of failure considered for the containment in this study is liner leakage. Although, tendon and reinforcing bar failure could lead to a liner or structural failure, a quantitative model to incorporate the loss of ductility because of general corrosion, stress corrosion cracking, and hydrogen embrittlement of these components was not developed. The liner is expected to leak before tendons or reinforcing bar failure.

A literature review of corroded tendons was conducted to investigate whether the loss of ductility of degraded tendons could be quantified. Numerous references were found on degraded tendons. However, only a few offered quantitative data on the reduction of ductility. For corroded high-strength bridge wire, Barton et al. (2000) found a significant embrittlement and a degradation of the ultimate load that was in excess of what could be attributed to the loss of section. For ungalvanized wire, the strain at ultimate load decreased by 40% from the uncorroded condition to the specimen with the maximum corrosion exposure time. In addition, Lopes and Simões (1999) found that for prestress strands the number of bends for a reverse-bend test were reduced by as much as 50% for corroded specimens. Finally, Vehovar et al. (1998) found that for corroded tendon specimens removed from an actual motorway viaduct, the elongation went from approximately 6.0 to 2.0%. In addition, the number of bends in a reverse-bend test went from approximately 3.5 down to fewer than 1. The authors attributed this loss of ductility to stress corrosion cracking.

There is some disagreement in the literature about whether stress corrosion cracking and hydrogen embrittlement will lower the failure stress significantly. Cherry and Price (1980) suggested that hydrogen only assisted in the initiation of failure and that the failure would occur at nearly the ultimate tensile strength of the material. However, Parkins et al. (1982) found that failures frequently occurred at stresses of 50% of the fracture stress. Parkins et al. suggested that the reasons for the differences between their work and that work of Cherry and Price was that the test strain rates were not the same, the specimens were corroded in different solutions, and the Cherry and Price specimens were not notched.

Bergsma et al. (1977) present results for prestressing tendons subjected to a corrosive environment that had a reduction in the reverse-bend values of 40 to 80% for the degraded specimens. Their results show that the effect of hydrogen embrittlement can depend on the solution to which the specimens have been exposed. The authors suggest that the corrosive environments that the test specimens were subjected to are not necessarily realistic when compared to actual environments; therefore, the results cannot be used in service life predictions. However, the results show a strong influence of hydrogen embrittlement on the ductility of the prestressing tendons and that the failure levels can be considerably below the ultimate tensile strength of the tendons.

The research suggests that corrosion does cause a loss of ductility in the prestressing tendons. However, it is not always clear whether the loss of ductility is due to general corrosion on the surface of the tendons or due to hydrogen embrittlement or stress corrosion cracking. In the previous study of degraded liners by Cherry and Smith (2001), the degraded liner was considered to have the same properties as uncorroded material. This assumption was considered reasonable for low-strength low carbon steels. The degradation was accounted for with a loss of section ac

accompanied by a loss of ductility. However, for cases of stress corrosion cracking and hydrogen embrittlement (such as can be found in high strength steels, such as prestressing tendons), the degraded material does not have the same properties as the undegraded material. The degraded material will have a decrease in ultimate load-carrying ability along with a loss of ductility (and not necessarily a loss of section). Therefore, for prestressing tendons, a strain-based failure criterion considering a loss of section with a loss of ductility would be inadequate. Also, the failure of a tendon anchor could not be accounted for with this criterion because in these analyses the anchorage is not modeled explicitly.

In this study, the prestressing levels were lowered to simulate degraded tendons. The strains in the tendons were examined but were not included in a failure criterion. The influence that failed tendons or lower than expected prestressing levels has on the containment capacity was investigated by examining liner failure.

Determining failure of the containment requires monitoring the liner, reinforcing bars, and tendons closely. The FE analysis does not predict reinforcing bar, tendon, or liner failure. The results must be post-processed to determine whether and when a failure occurs.

A strain-based failure criterion was selected and applied to the liner. The failure is predicted to occur when the calculated strains exceed a critical value. Researchers such as Hancock and Mackenzie (1976), Mackenzie et al. (1977), and Mangoine (1982) have shown that the critical failure strain varies as the stress state changes and that this strain can be related to the stress state. The failure criterion applied to the liner in this study is the same as that applied by Cherry and Smith (2001) and uses “knockdown” factors to adjust uniaxial failure strain data to a failure value. There are three knockdown factors that have been considered and applied. The three factors are consistent with a previous study by Miller (1990).

The critical effective plastic strain at which failure is predicted to occur is determined as follows:

$$\epsilon_{\text{failure}} = \epsilon_{\text{uniaxial}} * f_1 * f_2 * f_3$$

where,

$\epsilon_{\text{failure}}$ = effective plastic strain level where failure is predicted to occur.

$\epsilon_{\text{uniaxial}}$ = strain at failure from a uniaxial tensile test.

f_1 = knockdown factor to account for multiaxial stress state,

$$= 1.648 * e^{-(\sigma_1 - \sigma_2 - \sigma_3) / \sigma_{\text{von}}}$$

f_2 = knockdown factor to account for the sophistication of the analysis model.

f_3 = knockdown factor to account for variable material properties.

σ_{von} = von Mises effective stress.

$\sigma_{1,2,3}$ = principal stress.

The relationship for the first “knockdown” factor is from Hancock and Mackenzie (1976). The factor is determined from the analyses and relates the triaxial state of stress to the failure strain.

The second factor accounts for how much detail is incorporated in the FE model. For example, the element size in the mesh and missing structural details in the model affect the accuracy of the FE prediction. This factor approaches 1.0 as the mesh size becomes small and includes all the structural details. The value chosen in this study was determined by reviewing the detail included in the FE model in the critical failure region, and analytical results such as the strain gradient in the critical region.

The third factor accounts for variability in the material properties. Since the liner material is the same as that used by Cherry and Smith (2001), the same value for the f_3 factor was used for the liner. This value was chosen from the variation in the material properties found for tensile tests of the liner material. It was found that the elongation for the material varied from the mean by 22%.

In the previous study by Cherry and Smith (2001) knockdown factors were chosen for the lower-bound, best estimate, and upper-bound cases. However, in this study, only lower-bound estimates of the knockdown factor were used. This approach was chosen because it was thought that the failure criteria were not accurate predictors of a failure pressure but were the best option for a failure indicator and comparative examination of the impact degradation has on the liner stress state.

There are several shortcomings of the failure criteria with respect to this study. The FE model does not include details of the liner-to-concrete attachments. This is the likely location for a liner leakage failure. The failure criteria were not applied to the tendons or reinforcing bars, and cannot account for stress corrosion cracking or hydrogen embrittlement. Therefore, a low value for the knockdown factor for analysis sophistication must be chosen, and a reasonable upper-bound value would be difficult to choose.

These failure criteria allow only a study of the impact that lowering prestressing levels has on the triaxial state of stress in the global liner behavior, whereas the actual failure is likely governed by the triaxial state of strain at a local discontinuity. Also, this failure controlling discontinuity is likely influenced by a global deformed shape of the containment vessel, which can be accurately predicted only by a 3D model of the complete containment, including at least the major penetrations. The triaxial state of stress examined by the failure criteria in this study is an indicator of conditions where a local liner discontinuity could become critical. As a result, the failure indicator suggests conditions that would be more receptive to a failure. Thus, it is a measure of relative likelihood of failure and a good tool for examining the relative impact varying degrees of “degradation” have on the containment’s ultimate load-carrying capacity.

Values were chosen for two knockdown factors: $f_2 = 0.2$ and $f_3 = 0.78$. It should be emphasized that these values are based on engineering judgment and, therefore, depend on the analyst setting up the model. For example, some analysts may use a different material property factor value to account for affects of seasonal temperature changes or concrete creep. The intent is that the analysts consider each of these areas and determines an overall failure limit that is reasonable.

The American Society of Mechanical Engineers (ASME) code (ASME, 1992) gives a minimum uniaxial failure strain for elongation in a 20.3 mm (0.8 in.) gage length as 21% for ASTM A516 Grade 60 steel. Therefore, a value of 0.21 was used for $\epsilon_{\text{uniaxial}}$.

This page intentionally left blank.

3. Finite Element Runs and Results

3.1 Finite Element Runs

Tendon prestressing levels were varied as shown in Table 3-1 to investigate the effect that tendon degradation has on the ultimate capacity of the containment. To limit the scope of the analyses only the wall tendons were varied (except for one case of uniform degradation throughout the containment). The finite element (FE) model was analyzed, and the ultimate load-carrying capacity of the containment was evaluated by applying the failure criteria as described previously. Degradation was modeled by decreasing the level of prestressing (reduction of the tendon area was implemented only in Cases 9b and 15b).

Case 1 is the baseline failure case (no tendon degradation). Case 2 examines an incident where all the tendons have lower than expected prestressing levels (e.g., prestress loss due to higher than expected average temperature around the tendons). Cases 3 and 4 examine uniform tendon prestress loss for the hoop and vertical tendons respectively.

The cases examined allow an investigation of the ultimate load-carrying capacity of the containment with prestress loss during a loss of coolant accident (LOCA). A comparison of a group of degraded tendons located together versus degraded tendons that are distributed throughout the containment is possible. Also, a relative comparison of the hoop and vertical tendons can be made. Finally, a comparison of a 5% and 10% prestressing loss can be made to examine how the ultimate failure pressure of the containment changes with prestress loss.

There are 555 hoop tendons anchored at the six vertical buttresses in the containment vessel. This results in 185 hoop tendon rows along the height of the containment. For simplicity, all tendons were modeled as if they passed through the buttress. In the actual containment, the tendon rows would alternate between being anchored at the buttress and passing through the buttress to be anchored at the next buttress. The percent of tendons degraded is a percentage of these 185 hoop tendon rows. For the cases in this study, 5% hoop tendon degradation has 9 tendon rows degraded. For the 10% and 20% cases there are 19 and 37 tendon rows degraded, respectively.

There are 216 vertical tendons in the containment vessel. It was decided that the 30° segment of the model using symmetry was an accurate representation of a 60° segment of the complete containment. The hoop tendons span 120° segments of the containment (3 hoop tendons per tendon rows), while a vertical tendon has a tributary area of 1.67°. Therefore, the percentages listed in this study in regard to the vertical tendons are calculated from the number of tendons in a 60° segment of the containment ($216/6 = 36$). Thus, when 10% of the vertical tendons are degraded this means four of the tendons were degraded and for the 20% case 8 tendons were degraded. More precisely, this would result in 11.1% and 22.2% of the tendons degraded.

Table 3-1. Analysis Case

Case	Parameters
1	No degradation
2	Uniform loss of prestressing (vertical, hoop, and dome tendons)
3	Uniform loss of prestressing (hoop tendons)
4	Uniform loss of prestressing (vertical tendons)
5a	5% of the hoop tendons with 100% loss of prestressing (grouped at mid-height, tendons remain with no prestressing)
5b	5% of the hoop tendons with 100% loss of prestressing (grouped at mid-height, tendons removed, as if broken)
6	10% of the vertical tendons with 100% loss of prestressing (grouped at the center line)
7	20% of the vertical tendons with 50% loss of prestressing (grouped at the center line)
8	10% of the vertical tendons with 100% loss of prestressing (distributed)
9a	20% of the vertical tendons with 50% loss of prestressing (distributed)
9b	20% of the vertical tendons with 50% loss of area (distributed)
10	10% of the hoop tendons with 50% loss of prestressing (grouped at mid-height)
11	5% of the hoop tendons with 100% loss of prestressing (distributed)
12	10% of the hoop tendons with 50% loss of prestressing (distributed)
13	10% of the hoop tendons with 100% loss of prestressing (grouped at mid-height)
14	10% of the hoop tendons with 100% loss of prestressing (distributed)
15a	20% of the hoop tendons with 50% loss of prestressing (grouped at mid-height)
15b	20% of the hoop tendons with 50% loss of area (grouped at mid-height)

The analysis cases listed in Table 3-1 allow a number of comparisons to be made to gain insight into how prestressing loss can impact the ultimate load-carrying capacity of a containment vessel. The general categories of comparisons are as follows:

1. Uniform degradation (all, vertical, and hoop tendon) versus the baseline (no degradation case). (Cases 2, 3, and 4, versus Case 1.)
2. 100% loss of prestressing (tendons remain) versus 100% loss of prestressing (tendons removed). (Case 5a versus 5b.)
3. Vertical tendon comparisons:
 - a. 10% of tendons degraded 100% versus 20% of tendons degraded 50% (Cases 6 versus 7 and 8 versus 9a).
 - b. Degraded tendons grouped versus distributed (Case 6 versus 8 and 7 versus 9a).
 - c. Loss of area versus loss of prestress (Case 9a versus 9b).

4. Hoop tendon comparisons

- a. 5% of tendons degraded 100% versus 10% of tendons degraded 100% (Cases 5b versus 13 and 11 versus 14), 10% of tendons degraded 50% and 20% degraded 50% (Case 10 versus 15a).
- b. 5% of tendons degraded 100% versus 10% degraded 50% (Cases 5b versus 10 and 11 versus 12) and 10% degraded 100% versus 20% degraded 50% (Case 13 versus 15a).
- c. Degraded tendons grouped versus distributed (Cases 5b versus 11, 10 versus 12, and 13 versus 14).
- d. Loss of area versus loss of prestress (Case 15a versus 15b).

5. Hoop versus vertical tendon degradation.

These comparisons provide insight into the importance of uniform prestressing loss and degradation, prestressing loss versus loss of tendons, vertical tendon loss versus hoop tendon loss, and the influence of loss level versus ultimate load-carrying capacity of the containment.

3.2 Results

Tables 3-2 through 3-4 list results for the cases shown in Table 3-1. Each table gives the pressure at which the concrete reaches zero stress, the concrete cracks, reinforcing bars (rebars) yield, tendons yield, liner yields, and an ultimate failure pressure calculated using the failure criterion discussed earlier. Table 3-2 lists the results for the baseline and uniform degradation cases. Table 3-3 lists the results for the vertical tendon cases, and Table 3-4 lists the results for the hoop tendon cases.

Table 3-2. Results for the Baseline and Uniform Degradation Cases

		Case 1 (baseline)		Case 2		Case 3		Case 4	
		MPa	psi	MPa	psi	MPa	psi	MPa	psi
Concrete (0.0 stress)	Vertical	0.55	80	0.49	71	0.55	80	0.48	70
	Hoop	0.48	70	0.41	59	0.40	58	0.51	74
Concrete (cracks)	Vertical	0.90	130	0.83	120	0.90	130	0.67	97
	Hoop	0.62	90	0.54	79	0.55	80	0.63	91
Rebar (yields)	Vertical	1.10	160	1.10	160	1.10	160	1.10	159
	Hoop	0.97	141	0.96	139	0.97	141	1.01	147
Tendons (yields)	Vertical	1.15	167	1.15	167	1.14	166	1.15	167
	Hoop	0.97	141	0.99	144	0.98	142	0.96	139
Liner (yields)	Vertical	1.03	150	0.94	137	0.98	142	0.94	136
	Hoop	0.74	107	0.63	91	0.63	92	0.74	107
Liner Failure		1.01	146	1.00	145	1.01	146	1.01	147
Failure Strain (%)		2.4		2.3		2.3		2.3	

Table 3-3. Results for the Baseline and Degraded Vertical Tendons

		Baseline		Case 6		Case 7		Case 8		Case 9a		Case 9b	
		MPa	psi	MPa	psi	MPa	psi	MPa	psi	MPa	psi	MPa	psi
Concrete (0.0 stress)	Vertical	0.55	80	0.46	67	0.53	77	0.50	72	0.54	78	0.54	79
	Hoop	0.48	70	0.50	73	0.48	70	0.50	73	0.49	71	0.5	72
Concrete (cracks)	Vertical	0.90	130	0.76	110	0.82	119	0.69	100	0.69	100	0.69	100
	Hoop	0.62	90	0.63	91	0.62	90	0.62	90	0.63	91	0.63	91
Rebar (yields)	Vertical	1.10	160	1.16	168	1.10	160	1.10	160	1.09	158	1.09	158
	Hoop	0.97	141	1.01	147	0.96	140	1.02	148	1.01	147	1.02	148
Tendons (yields)	Vertical	1.15	167	1.12	162	1.12	162	1.10	159	1.14	166	1.13	164
	Hoop	0.97	141	0.97	141	0.96	140	0.96	139	0.96	140	0.96	140
Liner (yields)	Vertical	1.03	150	0.94	136	0.96	140	0.86	124	0.99	143	0.86	140
	Hoop	0.74	107	0.72	105	0.72	105	0.72	104	0.71	103	0.69	100
Liner Failure		1.01	146	1.01	146	1.01	146	1.00	145	1.01	146	1.01	146
Failure Strain (%)		2.4		2.3		2.3		2.2		2.3		2.3	

Table 3-4. Results for the Baseline and Degraded Hoop Tendons

		Baseline		Case 5a		Case 5b		Case 10		Case 11		Case 12		Case 13		Case 14		Case 15a		Case 15b	
		MPa	psi	MPa	psi	MPa	psi	MPa	psi	MPa	psi	MPa	psi	MPa	psi	MPa	psi	MPa	psi	MPa	psi
Concrete (0.0 stress)	Vertical	0.55	80	0.37	54	0.35	51	0.40	58	0.54	79	0.55	80	0.21	31	0.55	80	0.41	60	0.37	54
	Hoop	0.48	70	0.36	53	0.36	53	0.34	50	0.44	64	0.45	65	0.20	29	0.41	60	0.25	36	0.23	34
Concrete (cracks)	Vertical	0.90	130	0.56	81	0.55	80	0.55	80	0.76	110	0.90	130	0.35	51	0.83	120	0.90	130	0.56	81
	Hoop	0.62	90	0.48	69	0.48	70	0.48	70	0.55	80	0.55	80	0.34	50	0.55	80	0.34	50	0.35	51
Rebar (yields)	Vertical	1.10	160	1.10	159	0.95	138	1.09	158	1.03	150	1.10	160	0.76	110	0.96	139	1.10	160	0.76	110
	Hoop	0.97	141	0.94	136	0.88	129	0.89	129	0.94	137	0.95	138	0.69	100	0.87	126	0.83	120	0.69	100
Tendons (yields)	Vertical	1.15	167	1.15	167	1.06	154	1.15	167	1.08	156	1.15	167	0.90	130	1.01	146	1.15	167	0.82	119
	Hoop	0.97	141	0.88	128	0.84	122	0.83	120	0.90	130	0.95	138	0.68	99	0.83	120	0.99	144	0.62	90
Liner (yield)	Vertical	1.03	150	0.95	138	0.90	130	0.94	136	0.94	136	0.96	140	0.76	110	0.90	130	0.86	125	0.68	99
	Hoop	0.74	107	0.61	89	0.61	88	0.59	86	0.63	92	0.67	97	0.46	66	0.61	89	0.48	70	0.43	63
Liner Failure		1.01	146	1.00	145	0.92	133	1.01	146	0.94	136	1.00	145	0.77	112	0.79	114	0.99	144	0.71	103
Failure Strain (%)		2.4		2.3		2.3		2.3		2.4		2.3		2.3		2.4		2.2		2.3	

3.2.1 Results in Terms of Ultimate Capacity

The baseline no degradation case resulted in a calculated failure pressure of 1.01MPa (146 psi). As the results listed in Table 3-2 show, there is no significant influence on the calculated failure pressure when there is a 17.5% reduction in the prestressing levels. The reduction of prestressing levels has influence when the concrete reaches zero stress, cracks, and when the rebar and liner yield. However, there is little influence on the pressure at which the tendons yield.

Cases 5a and 5b (Table 3-4) were run to compare the cases of complete loss of prestressing versus loss of the tendons. In case 5a, 5% of the tendons do not have any prestressing. In case 5b, 5% of the tendons are completely removed. The tendons in case 5a can still behave as reinforcing bars. Case 5a experiences a very small decrease in calculated failure pressure. However, case 5b does show a 9% decrease in calculated failure pressure. Therefore, the case with the ten

dons removed (as if broken) was considered the critical case. Based on these results, this method was selected for use in the remaining 100% degraded cases.

Cases 6, 7, 8, 9a, and 9b (Table 3-3) were run to examine cases simulating degradation in the vertical tendons. As can be seen from the resulting calculated failure pressures (Table 3-3), degradation of the vertical tendons did not have a significant effect on the failure pressure for this LOCA condition. Thus, degrading the prestressing levels by 10% (either 10% degraded 100% or 20% degraded 50%) or reducing the area of 20% of the vertical tendons by 50% did not lower the calculated failure pressure.

Reduction of the prestressing or degradation of the hoop tendons showed a greater influence on the calculated failure pressure for the LOCA condition. Results of these analyses are shown in Table 3-4.

Removing 5% of the hoop tendons resulted in a decrease in the calculated failure pressure by approximately 9% while removing 10% resulted in a decrease in the calculated failure pressure by approximately 22%. However, when the prestressing levels were reduced by 50%, in either 10% or 20% of the hoop tendons, there was no significant impact on the calculated failure pressure. Therefore, a comparison of the cases where the hoop tendons were removed to those cases where the prestressing levels were only reduced shows that removing the tendons is much more significant.

Comparing cases 5b versus 11, 10 versus 12, and 13 versus 14, shows the significance of grouped versus distributed tendons. In all these cases, there is not a significant difference between the grouped and distributed tendons. Because the cases where the tendons were not removed have little effect on the calculated failure pressure (such as cases 10 and 12) this comparison likely should not be considered. In the other two comparisons where the tendons were degraded 100% (and removed), the grouped cases resulted in approximately 2% lower failure pressure.

The final comparison that was made for the degraded hoop tendon cases examined reducing the area of the tendon (keeping the prestressing level the same) and reducing the prestressing. The cases examined had 20% of the hoop tendons degraded 50% (Case 15a) compared to 20% of the hoop tendons with a 50% reduction of area (Case 15b). The case with the prestressing reduced to 50% showed only a 1.5% reduction in calculated failure pressure (which is consistent with other cases where the tendons were not removed), while the case where the area was reduced 50% showed nearly a 30% decrease in the calculated failure pressure.

When reviewing the impact on the calculated failure pressure in the cases where the tendons were removed (as if broken), there is a significant finding. When the tendons remained, and had load carrying capacity, there was not a significant impact on the calculated failure pressure. Reducing the tendon area while keeping the prestressing levels constant, also had a significant impact on the calculated failure pressure.

3.2.2 Other Trends

Failure pressure as calculated for this study is significant, especially when considering design margin and the ultimate capacity of prestressed containment vessels. However, it is not the only measure of containment behavior. Concrete cracking, rebar, liner, and tendon yielding, are also significant factors.

The pressure values reported in Tables 3-2 through 3-4 for the concrete reaching zero stress, concrete cracking, rebar yielding, and hoop tendons yielding were for locations in the model where the stress values were recorded for calculation of the failure criteria. This is the location where the highest liner stresses were found near completion of the FE calculations. The values reported for the yielding of the vertical tendons were at the location of the highest tendon stresses.

In general, these results show that the concrete will reach zero stress and crack sooner in the directions that the tendons lose their prestressing. For the cases shown in Tables 3-2 through 3-4, where there was uniform degradation (and no tendons were removed, only prestressing reduced), the pressure at which the tendons and rebar yield did not change significantly from the baseline case.

The failure locations of these models were not at concentrated locations. In general they were at approximately the mid-height of the cylinder wall. As the results in Tables 3-2 through 3-4 demonstrate, even though the concrete reaches zero stress, concrete cracks, rebar, tendons, or liner yield, at a lower pressure, it does not necessarily result in a lower calculated failure pressure. The stresses can redistribute prior to reaching critical levels.

3.2.3 Observations

It is important to reiterate that the analyses conducted for this study are best viewed as a relative comparison of the impact of reduced prestressing or degraded tendons on the ultimate load-carrying capacity of the containment vessel. Accurate failure prediction would require a more detailed analysis. Also, it is important to remember that the containment is designed for many more loading conditions than just a LOCA. From this study's results, it would appear that the vertical tendons have very little influence on the ultimate capacity of the vessel. However, for other loading conditions, such as seismic, the vertical tendons could have much more significant.

To verify that the tendons were not failing prior to the predicted failure of the liner, the strains in the tendons were examined relative to the predicted failure pressure from the failure criteria. Even in cases where tendons were removed, the remaining tendons were not at strain levels where failure was considered likely. However, if there were hydrogen embrittlement or stress corrosion cracking, the remaining tendons might fail at much lower strains. As discussed earlier, the failure criteria used in this study did not account for this type of phenomenon.

The model used in these analyses was a simplification of an actual structure. The vertical tendons did not account for friction, while the hoop tendons were modeled as rebar (bonded continuously to the concrete). The connections between the liner and the concrete were not included in the model.

If a containment vessel does not uniformly displace as pressure increases, strains likely will build up at one of the liner anchors. Therefore, this would be a likely location for a liner tear during a LOCA (in addition to penetrations or at material discontinuities, including welds). This FE model did not include either liner anchors or penetrations.

The pretest analysis of a 1:4-scale prestressed concrete containment vessel model (Dameron et al., 2000) found that frictional variation along the tendons and varying prestressing losses could significantly impact the deformed shape of a containment. The deformed shape will influence the strain build up at liner anchors. Therefore, for a FE model to more accurately predict the failure of the containment vessel, a method for incorporating this behavior must be included. When this 1:4-scale model was tested, the liner did fail at liner weld seams.² When a containment vessel globally deforms under a pressure loading, the liner anchors create strain discontinuities that can build up at regions such as the liner anchors or welds. The results from the 1:-scale model test supports the importance of accounting for these details in an FE model used to predict the ultimate load-carrying capacity of a containment vessel.

² Results of the tests of the 1:4-scale model of the prestressed concrete containment vessel tested at Sandia National Laboratories will be published at a future date.

This page intentionally left blank.

4. Conclusions

Despite some of the structural details that were not included in the finite element models, as discussed in previous sections, there are a number of conclusions that can be drawn.

1. For the LOCA analyzed in this study, the vertical tendons did not have a significant impact.
2. The uniform reduction of prestressing (all tendons, vertical tendons, and hoop tendons) did not result in a significant change in failure pressure from the baseline case (although the concrete cracked at a lower pressure).
3. The cases when the prestressing was reduced to zero, but the tendons remained at full strength, did not result in a significant impact on the calculated failure pressure.
4. The cases where the hoop tendons were completely removed resulted in the most significant decrease in calculated failure pressure.
5. When the degraded tendons were grouped together (as opposed to being uniformly distributed), there was approximately a 2% lower failure pressure compared to cases where the degraded tendons were distributed.

A future study is planned to examine the degradation of containment vessels in a risk-informed methodology. The study will attempt to build upon what was learned in this and previous studies (Cherry and Smith, 2001, Cherry et al., 2001³) to attempt an integrated assessment of containment degradation and review of the plant-licensing basis considering degradation as a temporary change in the plant-licensing condition.

³ Cherry et al. 2001 (in press). Aging Management and Performance of Stainless Steel Bellows in Nuclear Power Plants. Albuquerque, NM: Sandia National Laboratories.

This page intentionally left blank.

5. References

- ABAQUS/Standard User's Manual, Version 5.7*. 1997. Pawtucket, RI: Hibbit, Karlsson & Sorenson, Inc.
- ANACAP-U User's Manual, Version 2.5*. 1997. ANA-QA, 118. San Diego, CA: ANATECH Corp.
- Ashar, H., Naus, D., and Tan, C.P. 1994. "Prestressed Concrete in U.S. Nuclear Power Plants (Part 1)," *Concrete International*, May, 30–34.
- ASME (American Society of Mechanical Engineers). 1992. *Boiler and Pressure Vessel Code*. Section II, Part A, pp. 655–656. New York, NY: American Society of Mechanical Engineers.
- Barton, S.C., Varmaas, G.W., Duby, P.F., West, A.C., and Raimondo, B. 2000. "Accelerated Corrosion and Embrittlement of High-Strength Bridge Wire," *Journal of Materials in Civil Engineering*, Vol. 33, pp. 33-38.
- Bergsma, F., Boon, J.W., and Etienne, C.F. 1977. "Endurance Tests for Determining the Susceptibility of Prestressing Steel to Hydrogen Embrittlement," *Heron*, Vol. 22, no. 1, 46–71.
- Butler, T.A., and Fugelso, L.E. 1982. *Response of the Zion and Indian Point Containment Building to Severe Accident Pressures*. NUREG/CR-2569, LA-9301-MS. Los Alamos, NM: Los Alamos National Laboratory.
- Cherry, B.W., and Price, S.M. 1980. "Pitting, Crevice and Stress Corrosion Cracking Studies of Cold Drawn Eutectoid Steels," *Corrosion Science*, Vol. 20, 1163–1183.
- Cherry, J.L., and Smith, J.A. 2001. *Capacity of Steel and Concrete Containment Vessels with Corrosion Damage*. NUREG/CR-6706, SAND2000-1735. Albuquerque, NM: Sandia National Laboratories.
- Dameron, R.A., Zhang, L., Rashid, Y.R., and Vargus, M.S. 2000. *Pretest Analysis of a 1:4-Scale Prestressed Concrete Containment*. NUREG/CR-6685, SAND2000-2093. Albuquerque, NM: Sandia National Laboratories.
- Fatigue Technology, Inc. 1988. Sandia High Temperature Tensile Test Report. FTI Test Report 8057-1. Seattle, WA: Fatigue Technology, Inc.
- Hancock, J. W., and Mackenzie, A. C. 1976. "On the Mechanisms of Ductile Failure in High-Strength Steels Subjected to Multi-Axial Stress States," *Journal of Mechanics and Physics of Solids*, Vol. 24, 147–169.
- James, R.J., Zhang, L., Rashid, Y.R., and Cherry, J.L. 1999. "Seismic Analysis of a Prestressed Concrete Containment Vessel Model." NUREG/CR-6639, SAND99-1464. Albuquerque, NM: Sandia National Laboratories.

- Lopes, S.M.R., and Simões, L.M.L.P. 1999. "Influence of Corrosion on Prestress Strands," *Canadian Journal of Civil Engineering*, Vol. 26, No. 6, 782–788.
- Mackenzie, A. C., Hancock, J. W., and Brown, D. K. 1977. "On the Influence of State of Stress on Ductile Failure Initiation in High Strength Steels," *Engineering Fracture Mechanics*, Vol. 9, 167–188.
- Mangoine, M. J. 1982. "Creep-Rupture Behavior of Weldments," *Welding Journal Research Supplement*, Vol. 61, no. 2, American Welding Society.
- Miller, J. D. 1990. *Analysis of Shell-Rupture Failure Due to Hypothetical Elevated-Temperature Pressurization of the Sequoyah Unit 1 Steel Containment Building*. NUREG/CR-5405, SAND89-1650. Albuquerque, NM: Sandia National Laboratories.
- Norris, W.E., Naus, D.J., and Graves III, H.L. 1999. "Inspection of Nuclear Power Plant Containment Structures," *Nuclear Engineering and Design*, Vol. 192, 303–329.
- NRC (Nuclear Regulatory Commission). 1990. Determining Prestressing Forces for Inspection of Prestressed Concrete Containments. Regulatory Guide 1.35.1, July 1990. Washington, DC: NRC.
- NRC. 1999. Degradation of Prestressing Tendon Systems in Prestressed Concrete Containments. Information Notice No. 99-10, Rev. 1, October 1999. Washington, DC: NRC.
- Parkins, R.N., Elices, M., Sanchez-Galvez, V., and Caballero, L. 1982. "Environment Sensitive Cracking of Pre-Stressing Steels," *Corrosion Science*, Vol. 22, no. 5, 379–405.
- Rashid, Y. R. 1968, "Ultimate Strength Analysis of Prestressed Concrete Pressure Vessels," *Nuclear Engineering and Design*, 7, 334–344.
- Shah, V.N., and Hookham, C.J. 1998. "Long-Term Aging of Light Water Reactor Concrete Containments," *Nuclear Engineering and Design*, Vol. 185, 51–81.
- Steinberg, E.P. 1995. "Probabilistic Assessment of Prestressing Loss in Pretensioned Prestressed Concrete," *PCI Journal*, Vol. 40, no. 6, 76–85.
- Vehovar, L., Kuhar, V., and Vehovar, A. 1998. "Hydrogen-Assisted Stress-Corrosion of Prestressing Wires in a Motorway Viaduct," *Engineering Failure Analysis*, Vol. 5, no. 1, 21–27.

DISTRIBUTION:

(10) Herman L. Graves
U.S. Nuclear Regulatory Commission
RES/DET/ERAB
TWFN/Mail Stop 10-L1
11545 Rockville Pike
Rockville, MD 20852

(1) Dr. James F. Costello
U.S. Nuclear Regulatory Commission
RES/DET/ERAB
TWFN/Mail Stop 10-L1
11545 Rockville Pike
Rockville, MD 20852

1	MS	0736	T.E. Blejwas, 6400
1		0744	D.L. Berry, 6420
1		0744	M.F. Hessheimer, 6420
1		0744	V.K. Luk, 6420
1		0744	E.W. Klamerus, 6420
5		0744	J.A. Smith, 6420
15		0744	Dept. 6420 Resource Room
1		9018	Central Technical Files, 8945-1
2		0899	Technical Library, 9616
1		0612	Review & Approval Desk, 9612 For DOE/OSTI